Journal of the European Ceramic Society **8** (1991) 279–283

Oxidation Behavior of SiC–AlN Ceramic Materials

M. Landon, P. Goeuriot & F. Thevenot*

Laboratoire Céramiques Spéciales, Ecole Nationale Supérieure des Mines de Saint-Etienne, 158, cours Fauriel, 42023 Saint-Etienne, Cédex 2, France

(Received 18 December 1990; revised version received 3 May 1991; accepted 10 May 1991)

Abstract

This paper describes the oxidation behavior of monophased 2H solid solution SiC–AlN materials. Oxidation behavior of three compositions, 30, 50 and 80 wt% SiC, is investigated. Oxidation experiments are carried out in the temperature range of 1450 to 1600°C under pure oxygen atmosphere. The starting oxidation temperature of monophased SiC–AlN compounds is higher than 1450°C, whereas the oxidation temperatures of SiC and AlN start at a temperature of 800–1000°C.

A thermogravimetric study of the oxidation kinetics does not allow the determination of reaction mechanisms, gaseous species being trapped beneath oxides scale. The discontinuous escape of gas disrupts this layer, thus disturbing the recording of the weight measurement.

In dieser Arbeit wurde das Oxidationsverhalten einphasiger 2H SiC–AlN-Mischkristalle untersucht. Für die Versuche wurden drei verschiedene SiC-Gehalte von 30, 50 und 80 Gew.% ausgewählt. Die Oxidationsversuche wurden im Temperaturbereich von 1450 bis 1600°C in reinem Sauerstoff durchgeführt. Der Beginn der Oxidation liegt bei den einphasigen SiC–AlN-Verbindungen über 1450°C. Die Oxidation reinen SiC und AlN hingegen beginnt bereits im Temperaturbereich von 800 bis 1000°C.

Die thermogravimetrische Untersuchung der Oxidationskinetik erlaubt eine Bestimmung der Reaktionsmechanismen nicht, da entsprechende gasförmige Reaktionsprodukte unter der Oxidhaut nicht entweichen können. Das diskontinuierliche Entweichen des Gases zerstört diese Schicht und stört somit eine kontinuierliche Messung des Probengewichts.

Le comportement à l'oxydation des matériaux SiC–AlN se présentant cristallographiquement sous forme de solution solide 2H a été étudié. Trois compositions 30%, 50% et 80% en poids de SiC ont été retenues. Le comportement face à l'oxydation de nos matériaux a été suivi dans une gamme de température allant de 1450 à 1600°C sous atmosphère d'oxygène. L'oxydation débute à une tempèrature supérieure à 1450°C alors que les températures de début d'oxydation de SiC et de AlN sont de l'ordre de 800–1000°C.

L'étude cinétique par suivi thermogravimétrique ne permet pas de dégager de mécanismes réactionnels, dans la mesure où des espèces gazeuses sont piégées dans la couche d'oxydes. L'échappement discontinu de ces gaz, qui entraîne une rupture de la couche, perturbe l'enregistrement de la variation de masse.

1 Introduction

High-temperature applications have promoted considerable interest in the evaluation of oxidation behavior of silicon carbide. Most of these studies are conducted using powdered materials but some also use wafers, single or polycrystals, or 6H SiC polytype sintered or hot-pressed materials. This could explain the scattered values of the energy of oxidation, varying from 84 to 498 kJ mol^{-1}.[1] The excellent oxidation resistance of SiC is well known in the temperature range of 1000 to 1600°C, caused by the formation of a protective silica layer. The SiO_2 film may be amorphous or of the cristobalite form depending on the oxidation temperature. There is no general agreement regarding the rate-controlling process and the diffusing species: interstitial oxygen atoms,[2,3] ions[4,5] or molecules,[6–9] vacancies,[10] silicon atoms,[11] or SiO, C, CO and CO_2[12,13] appear at the internal interface SiC–SiO_2 and move to the

* To whom correspondence should be addressed.

Journal of the European Ceramic Society 0955-2219/91/$3.50

atmosphere. However, compiled results by Motzfeldt[6] and Norton's work[8] show that the parabolic law is related to the permeation of molecular oxygen through the growing SiO_2 scale. Oxygen partial-pressure dependence seems to be related to the oxidizing temperature[2,14] and the origin of the diffusing species.[15] Oxidation rate changes are observed when partial crystallization of the silica layer occurs. The experiments indicate that scale ruptures such as cracks[2] or bubble formation[13] take place with subsequent increase of oxidation. Investigations on oxidation resistances of SiC and AlN have been carried out in oxygen, steam and steam–oxygen, CO or CO_2 atmospheres.

The oxidation reaction of AlN[15–19] is less studied than the oxidation of SiC. The starting oxidation temperature of AlN powder is 700°C. A protective α-alumina film is formed; its thickness depends on the oxidation temperature.[16] In a first step oxidation exhibits a linear growth rate, when the activation energy is 218 kJ mol^{-1}, corresponding to the breaking of atomic bonds (226 kJ mol^{-1}). In the second step, in the temperature range of 1100–1300°C, a parabolic law is observed with an energy of 172 kJ mol^{-1}, corresponding to the oxygen diffusion. This energy depends on the impurity amounts and can vary from 100 to 372 kJ mol^{-1}. The oxidation of hot-pressed AlN samples starts at 1200°C but the degree of reaction α is low until a temperature of 1400°C is reached.[17] The literature does not give any study of the oxidation of a solid solution SiC–AlN–2H.

2 Experimental Procedure

2.1 Starting materials

Commercial powders of β-SiC and AlN (grades B10 and B, respectively, from Starck, Berlin) were well dispersed in a slurry, using magnetic stirring and ultrasonic apparatus; after drying, powder mixtures were hot-pressed in a graphite die under nitrogen at 2150°C for 45 min.[18,20] Three compositions were studied:

A80: 80 wt% of SiC and 20 wt% of AlN
A50: 50 wt% of SiC and 50 wt% of AlN
A30: 30 wt% of SiC and 70 wt% of AlN

No sintering additives were used. Samples have a density higher than 99% d_{th}.

The X-ray phase analysis was investigated in the range $2\theta = 25$–$75°$ with a low speed ($0{\cdot}5\ 2\theta$ min^{-1}) using a linear detector, Elphyse (window width of 12 mm); Cu$K_\alpha = 1{\cdot}5418$ Å and a nickel filter were used.

Both samples exhibited 2H solid solution single phase; some traces of 6H and 3C polytypes may be detected.[18,20] Using TEM determinations,[19,20] the mean grain sizes were determined (A80: $<1\ \mu$m; A50: 1–2 μm; A30: 5–6 μm); small alumina inclusions were found in A80, and small intergranular glassy phases and alumina inclusions were found in A30 and A50 AlN-rich samples.

2.2 Oxidation studies

Monophased 2H SiC–AlN samples were cut into platelets of $15 \times 15 \times 1$ mm^3 then polished up to 3 microns diamond paste. The oxidation of fully densified hot-pressed platelets was followed by thermogravimetric analysis using a Netzsch STA 429 thermobalance, which allowed a continuous measurement of weight gain versus time. The heating rate was 10°C min^{-1} under argon. When the oxidizing temperature was reached, the argon gas was substituted by oxygen gas (flow rate 3 liters min^{-1}). The mass variations were then recorded.

As only weak oxidation appears at 1200°C, oxidation experiments were carried out at higher temperatures ($T > 1450$°C). The degree of reaction α is defined as follows:

$$\alpha = \Delta m(t)/\Delta m(t = \infty)$$

where $\Delta m(t = \infty)$ is the theoretical weight variation for the total oxidation.

3 Results and Discussions

3.1 Thermogravimetry

Figures 1–3 show the variation of the degree of reaction versus time. For each sample the reaction rate decreases with time except for the upper temperature of oxidation (1600°C) for poor SiC materials (A30). For high SiC content (A80) the

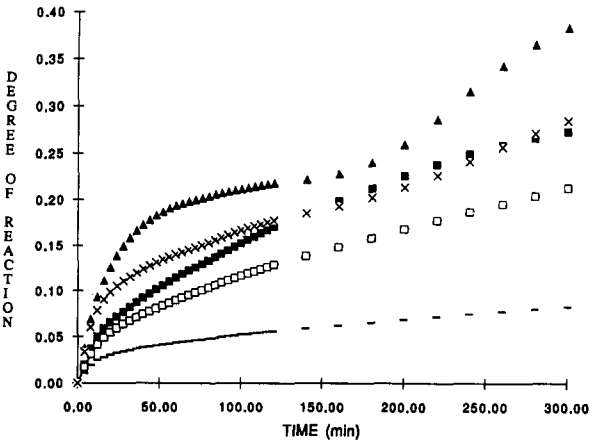

Fig. 1. Degree of reaction of sample A30 (30% SiC). —, 1450°C; □, 1500°C; ■, 1550°C; ×, 1570°C; ▲, 1600°C.

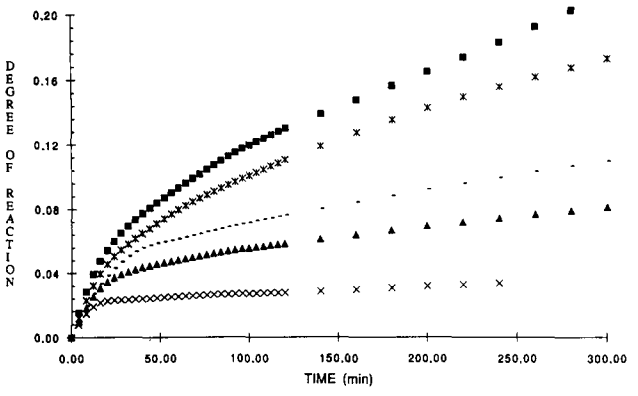

Fig. 2. Degree of reaction of sample A50 (50% SiC). ×, 1450°C; ▲, 1500°C; —, 1525°C; ✳, 1550°C; ■, 1570°C.

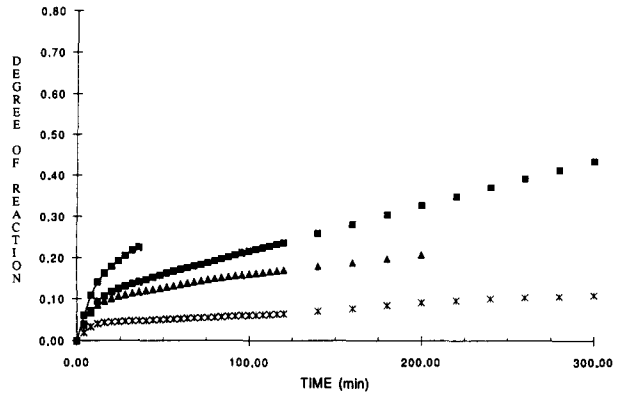

Fig. 3. Degree of reaction of sample A80 (80% SiC). ✳, 1550°C; ▲, 1570°C; ■, 1590°C; -■-, 1600°C.

recording must be stopped after some time of oxidation due to the explosion of bubbles at the surface of samples.

In order to determine if the oxidation phenomenon is controlled in the whole range of temperature by the same mechanism, it is necessary that each experimental curve is deduced by orthogonal affinity (scaling) from one or other of the curves.[21] In this case this affinity does not exist, therefore no oxidation kinetics explanation of the SiC–AlN (2H) solid solution can be given. In spite of that, diffusional laws ($\alpha^2 = f(t)$) have been verified during the first period ($t < 15$ min) but different phenomena occur, and the recording of the weight change is not a good way to determine the oxidation mechanism; thus such curves are not represented here. The study of the oxidized layer thickness should be a better way of investigation.

3.2 X-Ray analysis

The nature of the oxide film caused by oxidation phenomenon is analyzed by X-ray diffraction. The oxide layer is very thin because the substrate diffraction peaks are still detected (Fig. 4). The identification of other peaks shows that mullite or sillimanite phase is formed. According to the SiO_2–Al_2O_3 phase diagram, cristobalite and mullite phases should be pointed out, but from literature the

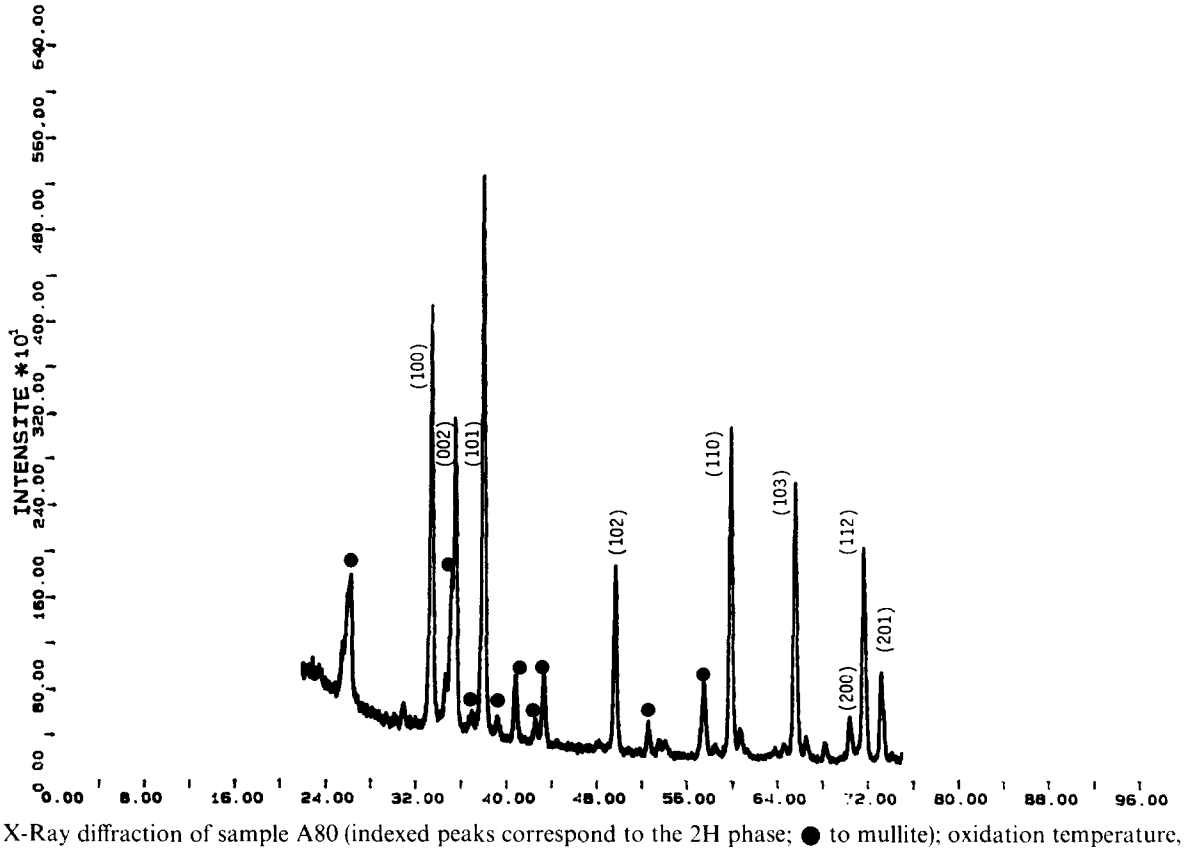

Fig. 4. X-Ray diffraction of sample A80 (indexed peaks correspond to the 2H phase; ● to mullite); oxidation temperature, 1570°C.

phase transformation sillimanite → mullite occurs as soon as a temperature of 1300°C is reached. In these experiments no cristabalite formation occurs but a vitreous phase is revealed because of the diffusion of the XRD beam at low angles.

3.3 SEM analysis

Oxide surfaces are quite different according to the different materials. Surface platelets of A80 sample are covered by a vitreous scale when oxidation occurs at 1525–1600°C. All surfaces exhibit an extensive bubble formation (Fig. 5), but crystallized zones located between amorphous places and bubbles (Fig. 6) or emerging out the glassy scale are seen as soon as an oxidizing temperature of 1550°C is reached. A local analysis of these crystallized places indicates a 'Si/(Si + Al)' ratio of 60% whereas a ratio of 95% is detected on vitreous places. This ratio is higher than the initial value of 80%. The large bubble eruptions are responsible for the lack of balance. Bubble formation, which has been observed by several researchers, can be attributed to the formation of the carbonaceous species (CO, CO_2), N_2 and SiO gas molecules. The oxide film interferes with the escape of gas molecules involved in the bubbles formation. So, when the viscosity is low, medium pressures due to the gas molecules storage are accommodated, but when the gaseous species pressures are too high scale disrupts appear, allowing their departure. The substrate is once again in contact with the oxygen atmosphere and strong weight gains are newly recorded (Fig. 1).

Oxidation surfaces of A50 and A30 samples are quite similar. Crystallization occurs as soon as an oxidizing temperature of 1450°C is applied. The vitreous phase is less abundant in A30 and A50 samples than in A80 sample but still present. Junction between the fine crystalline features (2–5 μm long) is assured by the glassy phase (Fig. 7). Vitreous bubbles are not seen but crystallized humps are visible (Fig. 8). The crystallized scale seems to prevent the gaseous molecules escape with more efficiency than the vitreous film, but when the gas pressure is too strong the crystallized protuberances break out (Fig. 9); then the oxidation of A30 sample led to 1570°C and 1600°C starts again (Fig. 1).

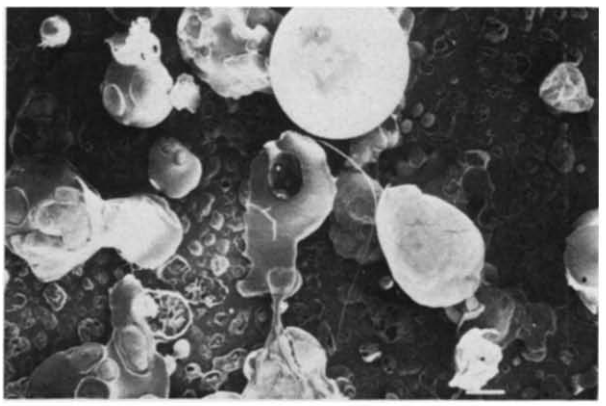

Fig. 5. Bubble formation (bar = 100 μm); A80 sample, T = 1525°C.

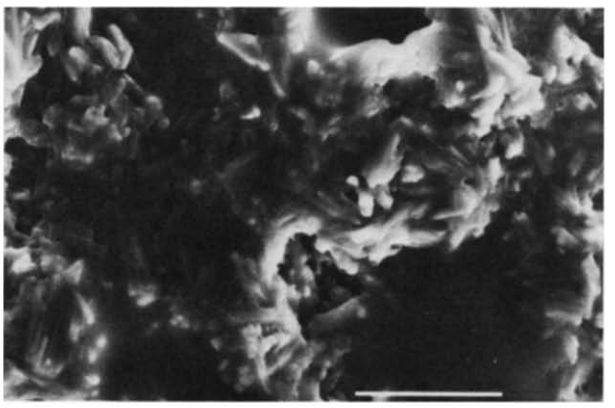

Fig. 7. Fine features embedded in a vitreous phase (bar = 10 μm); A50 sample, T = 1500°C.

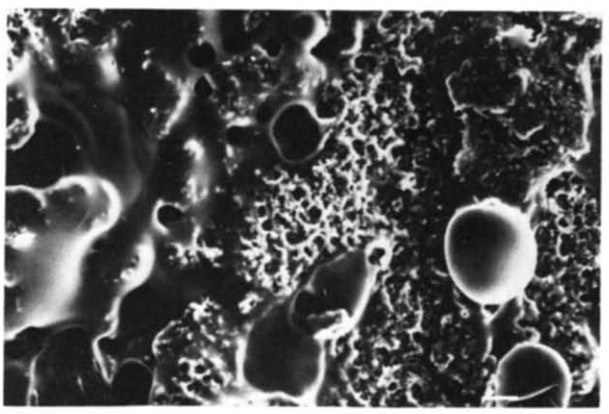

Fig. 6. Vitreous and crystallized phases and bubbles (bar = 100 μm); A80 sample, T = 1500°C.

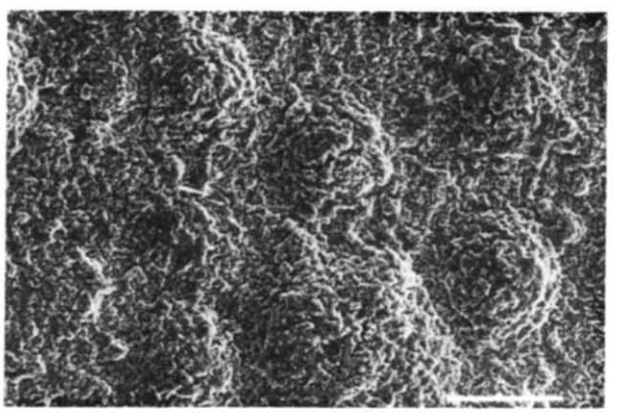

Fig. 8. Crystallized film (bar = 100 μm); A50 sample, T = 1550°C.

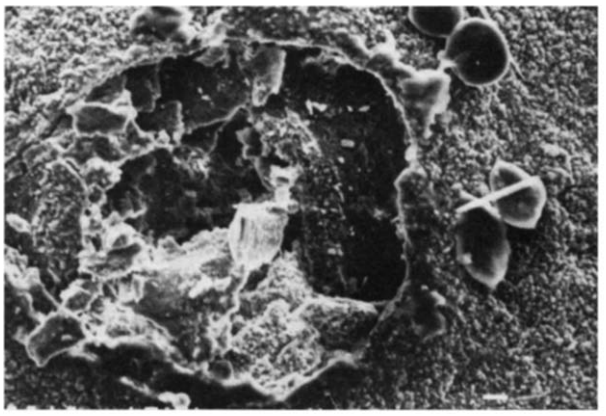

Fig. 9. Film disrupts (bar = 10 μm); A30 sample, $T = 1550°C$.

4 Conclusions

The oxidation behavior of hot-pressed 2H SiC–AlN solid solution was investigated from 1450 to 1600°C but no kinetics law could be applied.

A diffusional mechanism should exist at the beginning of the reaction. The oxidation of SiC–AlN samples is perhaps controlled during this period by the diffusion of species such as N_2, CO_2, CO or SiO molecules created at the internal interface and trapped under the oxide scale. The oxide layer being constituted by crystalline mullite phase and silica or Si–O–N glassy phases, it may disrupt (be broken) according to the value of its viscosity.

Up to 1550°C, at the beginning of the oxidation, the materials having the higher SiC contents (50–80% SiC) are the more resistant, but for higher oxidation temperatures the oxidation behavior of compounds with high AlN content is better, because vitreous bubble explosions due to the low viscosity of silica layer cannot occur.

References

1. Costello, J. A. & Tressler, R. E., Oxidation kinetics of hot-pressed and sintered α-SiC. *J. Am. Ceram. Soc.*, **64** (1981) 327–31.
2. Hinze, J. W., Tripp, W. X. C. & Graham, H. C., The high temperature oxidation of hot-pressed silicon carbide. In *Mass Transport Phenomena in Ceramics*, ed. A. R. Cooper & A. H. Heuer. Plenum Publishing Co., NY, 1975, pp. 409–21.
3. Jorgensen, P. J., Wadsworth, M. E. & Cutler, I. B., Oxidation of silicon carbide. *J. Am. Ceram. Soc.*, **42** (1959) 613–16.
4. Jorgensen, P. J., Effect of an electric field on silicon oxidation. *J. Chem. Phys.*, **37** (1962) 874–7.
5. Jorgensen, P. J., Wadsworth, M. E. & Cutler, I. B., Effect of oxygen partial pressure on the oxidation of silicon carbide. *J. Am. Ceram. Soc.*, **43** (1960) 209–12.
6. Motzfeldt, T. K., On the rates of oxidation of silicon and silicon carbide in oxygen and correlation with permeability of silica glass. *Acta Chem. Scand.*, **18** (1964) 1596–606.
7. Deal, B. E. & Grove, A. S., General relationship for the thermal oxidation of silicon. *J. Appl. Phys.*, **36** (1965) 3770–8.
8. Norton, F. J., Permeation of gaseous oxygen through vitreous silica. *Nature (London)*, **191** (1961) 701.
9. Dietzel, A. & Oberlies, F. S., Über die Struktur des Quartzglases. *Glastechn. Ber.*, **30** (1957) 37–42.
10. Fowkes, F. M. & Hielscher, F. H., *ECS Meeting, Seattle, Extended Abstracts*, **78** (1978) 434.
11. Heuer, A. H., Ogbuji, L. U. & Mitchell, J. E., Microstructure of oxide scales on oxidized Si and SiC single crystals. *J. Am. Ceram. Soc.*, **63** (1980) 354–5.
12. Fitzer, E. & Ebi, R., *Kinetic Studies on the Oxidation of Silicon Carbide*, ed. R. C. Marschall & J. W. F. C. E. Ryan. University of South Carolina Press, Columbia, 1973, pp. 320–8.
13. Mieskowski, D. M., Mitchell, T. E. & Heuer, A. H., Bubble formation in oxide scales on SiC. *J. Am. Ceram. Soc.*, **67** (1984) C17–C18.
14. Narushima, T., Goto, T. & Hirai, T., High temperature passive oxidation of chemically vapor deposited silicon carbide. *J. Am. Ceram. Soc.*, **72** (1989) 1386–90.
15. Cooper, C. F., George, C. M. & Hopkins, S. W. J., Preparation and oxidation of aluminium nitride. *Spec. Ceram. Proc. Symp. Brit., Ceram. Research Assoc.*, **49** (1962) 49–79.
16. Taylor, K. M. & Lenie, C., Some properties of aluminium nitride. *J. Electrochem. Soc.*, **107** (1960) 308–14.
17. Lecompte, J. P., Contribution à l'étude du frittage sous charge du nitrure d'aluminium. PhD thesis, Limoges, France, March 1982.
18. Landon, M. & Thevenot, F., The SiC–AlN system. *Ceramics International*, **17** (1991) 97–110.
19. Xu, Y. R., Zangvil, A., Landon, M. & Thevenot, F., Microstructure and mechanical properties of hot-pressed SiC–AlN compositions. *J. Am. Ceram. Soc.*, in press.
20. Landon, M., Le système carbure de silicium–nitrure d'aluminium. PhD thesis No. 52TD, Ecole des Mines de Saint-Etienne, France, 8 February 1991.
21. Barret, P., *Cinétique Hétérogène*. Gauthier-Villars, Paris, 1973, p. 198.